COMPUTATIONAL MECHANICS 2022
37th conference with international participation
Srní
November 7 - 9, 2022

Sensitivity analysis of thermodynamical parameters on the thermal bowed rotor using 2D finite element model

J. Pařez [a], P. Kovář [b], T. Vampola [a]

[a] *Department of Mechanics, Biomechanics and Mechatronics, Faculty of Mechanical Engineering, Center of Aviation and Space Research, Czech Technical University in Prague; Technicka 4; 160 00, Prague 6; Czech Republic, Jan.Parez@fs.cvut.cz*
[b] *Department of Technical Mathematics, Faculty of Mechanical Engineering, Center of Aviation and Space Research, Czech Technical University in Prague; Technicka 4; 160 00, Prague 6; Czech Republic, Patrik.Kovar@fs.cvut.cz*

Numerical modelling of mechanical systems is a helpful tool for system behaviour analyses. There are several well-known commercial softwares that deal with different solution areas. When interdisciplinary tasks are solved, the possibility of using software is more limited. It is due to many differences in the specific field of solutions as structural analyses, temperature distribution, heat transfer, etc. Therefore, solvers based on finite element method (FEM) are limited to a narrow group of solvable problems for the most part or they are generalized to universal problems. For specific analyses of aircraft engine rotors, a FEM solver consisted of MATLAB scripts was developed where different types and scopes of the task are implemented. Optional choice of boundary and initial conditions are possible as well. This contribution deals with a sensitivity analysis of the basic thermodynamic parameters during the operation of the aircraft engine rotor and their influence on the structural analysis and, above all, the deformation of the system.

The problem of the thermal bow has been known and solved in the field of energy for a long time. Zhuo [7] introduced a new computational method for thermal bow predicting on heavy gas turbines. The subsequent vibrations affecting the safe operation during restart of the rotor system caused by the temperature bowed rotor were presented in several works, for example in Chatterton [1], Pennacchi [4], or Marinescu [2]. In the field of aircraft engines, the rotor thermal

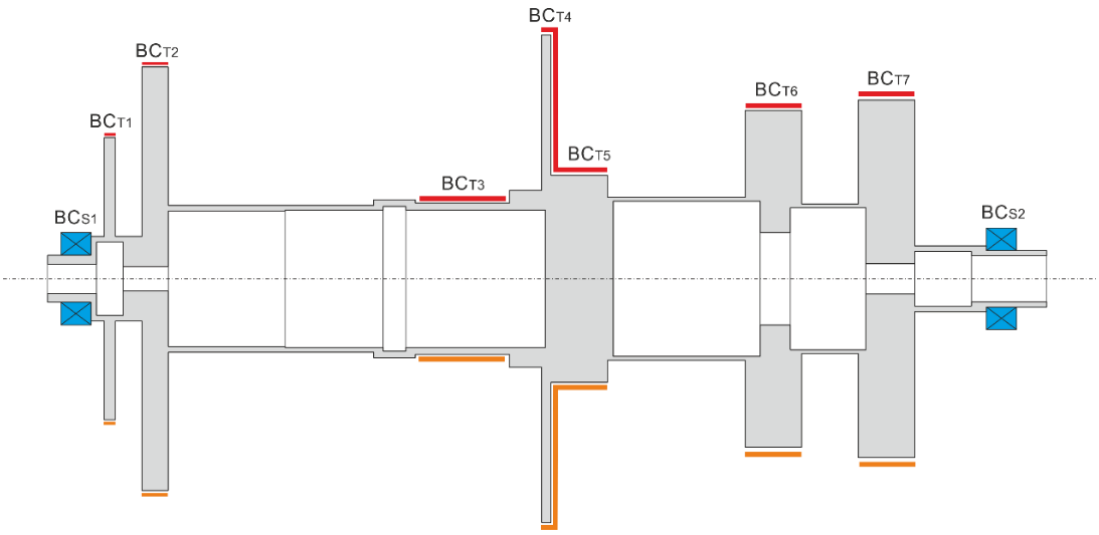

Fig. 1. Sketch of the turbine engine rotor system computational domain

deformation is very significant due to high temperature exposures and the radial clearance limitation which influences the efficiency. A significant contribution to research in this area was made by E.O. Smith in [5]. Last but not least contribution in thermal bow research, supplemented with experimental measurements by research at the Harbin Institute of Technology [6, 8].

Fig. 1 shows a sketch of simplified turbine aircraft engine rotor system computational domain including the location of prescribed boundary conditions. The two axial compressor discs on the right side are followed by a simplified model of the centrifugal compressor impeller in the centre of the rotor system. The generator turbine disc is located on the left side of the rotor system and ends with a disc of labyrinth seals.

According to the following table Table 1., initial and boundary conditions for temperature field distribution are prescribed. All listed values are given in degrees Celsius. Dirichlet boundary conditions are considered for surfaces with heat transfer and oil cooling. As mentioned above, locations of the boundary conditions are shown in the figure Fig. 1.

Table 1. Prescribed boundary condition for the turbine engine analysis

	BC_{T1}	BC_{T2}	BC_{T3}	BC_{T4}	BC_{T5}	BC_{T6}	BC_{T7}	BC_{S1}	BC_{S2}
Case 1	448	548	424	371	338	277	260	Pinned	Roller
	412	502	410	348	327	252	247		
Case 2	465	787	553	432	385	282	268	Pinned	Roller
	449	742	536	408	372	264	251		
Case 3	494	926	674	493	421	287	272	Pinned	Roller
	473	875	647	462	401	269	254		
Case 4	448	548	424	371	338	277	260	Pinned	Pinned
	412	502	410	348	327	252	247		
Case 5	465	787	553	432	385	282	268	Pinned	Pinned
	449	742	536	408	372	264	251		
Case 6	494	926	674	493	421	287	272	Pinned	Pinned
	473	875	647	462	401	269	254		

The rotor system is supported by two bearings BC_{S1} and BC_{S2}. In the analysis, variants when bearing displacement is possible are considered for Cases marked as 1 – 3 and the variant of a stuck bearing with a restriction to displacement for dilation for Cases denoted as 4 – 6. Furthermore, BC_{T1} – BC_{T7} represent the temperatures in significant areas divided into the upper and lower side when considering the inhomogeneous distribution of the temperature field due to the developed natural convection published in [3]. BC_{T7} and BC_{T6} represent the first two stages of the axial compressor. BC_{T4} to BC_{T5} represents the centrifugal compressor impeller. BC_{T3} is the area of the combustion chamber cooled by flowing fuel. BC_{T2} is the generator turbine wheel area and BC_{T1} stands for the temperature in the labyrinth seals.

Temperatures are considered for the turbine engine cooling when it is shut down after 5 minutes in three stable flight modes, i.e., idle mode, cruise mode and maximum take-off mode.

In the figure Fig. 2., there is a visualization of the calculated temperature field for the Case 6 representing the maximum take-off mode under the influence of the boundary conditions listed in the table Table 2. The deformation of the rotor without the possibility of axial dilation of the rotor system for the same case is shown in figure Fig. 3.

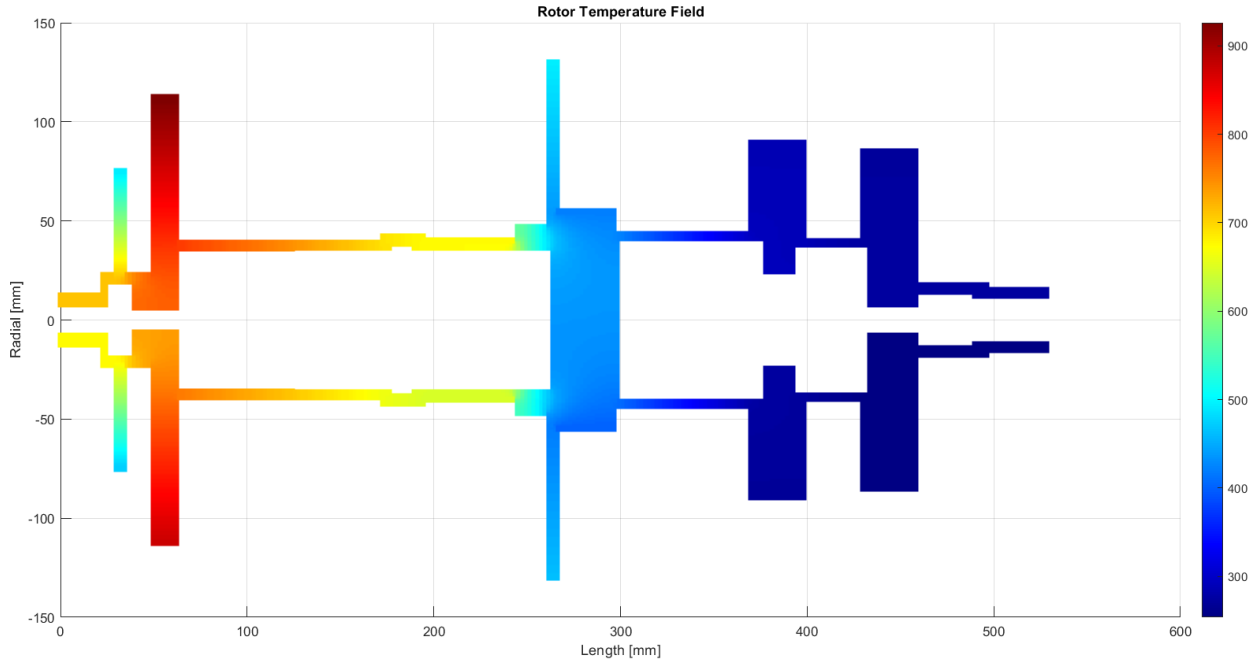

Fig. 2. Temperature field distribution on the turbine engine rotor system

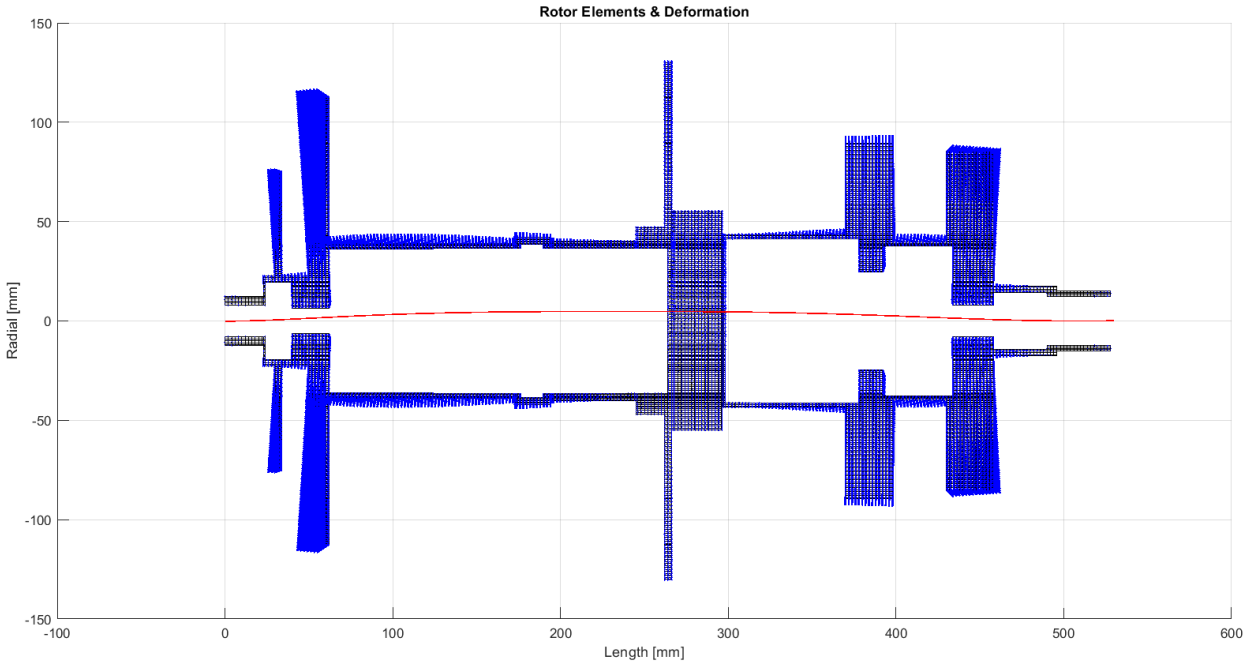

Fig. 3. Deformation and deflection distribution on the turbine engine rotor system

Fig. 2 shows the variable distribution of the temperature field due to heating from the flowing gases on the generator turbine as well as other structural nodes of the turbine engine. The asymmetric temperature field distribution between the upper and lower sides of the rotor is considered due to cooling by natural convection.

The asymmetry and inhomogeneous temperature field results in the rotor deformation shown in Fig. 3. Axial and radial components of the deformation are indicated by blue vector lines for each node of the computational mesh. Total deflection of the rotor centreline is plotted as a red curve, for clearer visibility this deflection is plotted as tenfold of this deformation.

The maximum rotor deflection, together with its position, are listed in Table 2 for all specified cases.

Table 2. Maximum deflection for specified cases

	Max. deflection [mm]	Max. deflection distance [mm]	BC_{S1}	BC_{S2}
Case 1	0.235	162	Pinned	Roller
Case 2	0.224	165	Pinned	Roller
Case 3	0.305	167.5	Pinned	Roller
Case 4	0.498	240	Pinned	Pinned
Case 5	0.483	238	Pinned	Pinned
Case 6	0.613	232.5	Pinned	Pinned

The resulting deflections of the rotor axis due to the temperature field distribution after shutting off the engine in the defined modes can be seen from Table 2. There is an increase in deflection with the increasing temperature difference of the asymmetric temperature field at higher speed mode. There is also a requirement for the functionality of the axial displacement of bearing which is also of key importance for the dynamic behaviour of the rotor system. The results show a dependence on the position of the maximum deflection, which is not much dependent on the selected mode respectively temperatures but dependent on the possibility of axial displacement of the bearing.

Acknowledgements

Authors acknowledge support from the ESIF, EU Operational Programme Research, Development and Education, and from the Center of Advanced Aerospace Technology (CZ.02.1.01/0.0/0.0/16_019/0000826), Faculty of Mechanical Engineering, Czech Technical University in Prague.

This work was supported by the Grant Agency of the Czech Technical University in Prague, grant No. SGS19/157/OHK2/3T/12.

References

[1] Chatterton, S., et al., An unconventional method for the diagnosis and study of generator rotor thermal bows, Journal of Engineering for Gas Turbines and Power 144(1) (2022) 011024.
[2] Marinescu, G., Ehrsam, A., Experimental investigation into thermal behavior of steam turbine components. Part 2 – Natural cooling of steam turbines and the impact on LCF life, ASME Turbo Expo Copenhagen, Denmark, 2012.
[3] Pařez, J., et al., Experimental and numerical study of natural convection in 3D double horizontal annulus, EPJ Web of Conferences, 2022, 264(1), ISSN 2100-014X.
[4] Pennacchi, P., Vania, A., Accuracy in the identification of a generator thermal bow, Journal of Sound and Vibration 274 (2004) 273-295.
[5] Smith, E., Neely, A., A study of cranking effectiveness as a treatment for rotor thermal bow in gas turbines, International Society of Airbreathing Engines (2019) 24025.
[6] Yuan, H.Q., et al. Dynamic characteristics of transient thermal starting up of a rotor system, Journal of Vibration and Shock 28 (2009) 33-37.
[7] Zhuo, M., et al. A new computational method for predicting the thermal bow of a rotor, Proceedings of the Institution of Mechanical Engineers, Part C: Journal of Mechanical Engineering Science (2019) 4372-4380.
[8] Zhu, X.Z., et al., Effects of steady temperature field on vibrational characteristics of a rotor system, Journal of Northeastern University 29 (2008) 113-116.